



## A burner to emulate condensed phase fuels



Y. Zhang<sup>a</sup>, M. Kim<sup>a</sup>, P.B. Sunderland<sup>a</sup>, J.G. Quintiere<sup>a,\*</sup>, J. de Ris<sup>b,1</sup>

<sup>a</sup> Dept. of Fire Protection Engineering, University of Maryland, College Park, USA

<sup>b</sup> FM Global, USA

### ARTICLE INFO

#### Article history:

Received 22 September 2015

Accepted 22 September 2015

Available online 30 September 2015

#### Keywords:

Burner  
Emulating  
Pool fires

### ABSTRACT

A gas-fueled burner with heat flux gages embedded in its porous surface is used to emulate condensed fuel flames. The measured heat flux, the flow rate of the fuel/inert mixture, and the burner surface temperature allow the emulation of the burning characteristics of condensed fuels. The burner is named the Burning Rate Emulator (BRE). It can burn a gaseous fuel at an effective heat of gasification matching the actual heat of gasification of condensed-phase fuels. It also can match other characteristics of the condensed-phase fuel by careful selection of certain properties of the gaseous fuel. These properties are the heat of combustion, the effective heat of gasification, the surface temperature, and the laminar smoke point. The BRE is shown to reasonably emulate steady burning of methanol, heptane, polyoxymethylene (POM) and polymethylmethacrylate (PMMA) burning in 50 mm diameter pools. It also can be used to emulate ignition and extinction. The results can be used to predict behavior at other conditions, such as burning with external radiant heating. The BRE can be extended to emulate steady burning under diverse conditions. The plausibility of the BRE is demonstrated and its limitations and difficulties are discussed. In particular, the difficulty of dealing with the actual surface heat flux distribution is examined. In general, the paper intends to demonstrate the attributes of a BRE.

© 2015 Elsevier Inc. All rights reserved.

### 1. Introduction

This study seeks to establish the burning conditions for condensed fuels using a gaseous burner. The burner conditions represent those of steady burning with the heat of gasification of the material as the principal fuel property. In addition three other properties are put forth to complete an emulation. They include the heat of combustion needed to control flame extent, re-radiation heat flux governing surface heat loss, and flame radiation represented by the laminar smoke point. These properties are hypothesized to establish the physical identity of the fuel its chemistry is not directly considered.

We seek to define the burning rate in terms of these four properties by using an emulator having a controlled gaseous fuel supply. The chemical nature of the gas is not modeled in respect to the real fuel's chemical composition. The Burning Rate Emulator (BRE) can be operated to simulate a condensed-phase fuel in steady burning. The results will depend on size, orientation, and environmental conditions; however, we will examine primarily burning in air.

The theory of steady burning for an evaporating condensed fuel is considered as the basis of the BRE. Although steady burning is not practical for many condensed fuels, the BRE can still give valuable insight on average. In other words, as wood would have a non-steady burning signature due to charring, its peak or overall average burning rate can be represented by an appropriate (usually a high) value for the heat of gasification. Steady burning (rate per unit area or burning flux) can be formulated in terms of a heat of gasification ( $L$ ) as

$$\dot{m}'' = \frac{\dot{q}_f'' - \dot{q}_r'' + \dot{q}_e''}{L}, \quad (1)$$

where the quantities are defined in the nomenclature. The heat of gasification for liquids is a thermodynamic property defined as

$$L = h_{vap} + c_p(T_v - T_\infty), \quad (2)$$

where  $h_{vap}$  is the heat of vaporization,  $c_p$  is the specific heat,  $T_v$  is the surface vaporization temperature, and  $T_\infty$  is the ambient temperature. The heat of gasification of polymers will involve more phases and transitions. As stated even charring materials, in time-average burning, can be couched in terms of a relatively high value of  $L$ .

The flame heat flux is controlled by convective and radiative components, and the surface re-radiation heat flux by the temperature of the vaporizing surface. In the case of the BRE, it is the

\* Corresponding author.

E-mail address: [jimq@umd.edu](mailto:jimq@umd.edu) (J.G. Quintiere).

<sup>1</sup> Retired.

### Nomenclature

$B$	$B \equiv [Y_{ox}\Delta h_c/r - c_p(T_v - T_\infty)]/L$ (dimensionless)	$\dot{q}_f''$	incident flame heat flux (kW/m <sup>2</sup> )
$c_p$	specific heat of gas (J/g K)	$\dot{q}_{rr}''$	surface radiative loss heat flux to ambient (kW/m <sup>2</sup> )
$h_c$	convective heat transfer coefficient (W/m <sup>2</sup> K)	$r$	stoichiometric mass oxygen to fuel ratio (g/g)
$\Delta h_c$	heat of combustion (kJ/g)	$T_v$	vaporization temperature (K)
$h_{vap}$	heat of vaporization (kJ/g)	$T_\infty$	ambient temperature (K)
$\dot{m}''$	burning rate (g/m <sup>2</sup> s)	$Y_{ox}$	ambient oxygen mass fraction (g/g)
$L$	heat of gasification (kJ/g)		
$\dot{q}_e''$	incident external radiative heat flux (kW/m <sup>2</sup> )		

burner surface temperature that gives the surface re-radiation. Heat flux gages in the burner surface record the flame heat flux, which includes both incident radiation and convection to the surface. With the measured gas flow rate of the burner, values of  $L$  can be determined from Eq. (1). While such values might seem simplistic, an effective  $L$ , which includes external heating, can define the enhancement conditions needed for that  $L$  to burn. By varying the gaseous fuel–inert mixture, the heat of combustion and the radiation character (specifically the laminar smoke point) can be varied. For a given configuration, a wide range of burning conditions can be readily established with the emulator (BRE).

But the development of the required net heat flux of Eq. (1) can present a challenge, and the control of a burner's surface temperature can be difficult. While the dilution of a gaseous fuel with an inert gas might match the heat of combustion and the smoke point of the emulated fuel, complete matching may only be approximately achieved.

The use of a burner to emulate combustion of solids and liquids has been used previously examined. Orloff and de Ris [1], Kim et al. [2], and de Ris et al. [3] pioneered the use of sintered metal burners for studying the steady burning of a planar condensed phase. Their burner used water cooling to obtain the needed heat flux, and thus the surface temperature was low. The water cooling also led to long equilibrium times. They examined mainly convective burning through the Spalding  $B$  number. For a given ambient condition, the  $B$  number is principally a function of the heat of gasification,  $L$ . The burning rate per unit area in purely diffusive or convective burning is also principally a function of the  $B$  number. Flame radiation and surface re-radiation disturb this simple dependence. However, the relatively simple dependence could be emulated by the de Ris burner, and is shown to follow laminar pure convective flame theory [1–3].

The use of a burner is imperfect, as it generally maintains a uniform velocity over its surface. Boundary layer or pool burning, even for pure convection, will have a distribution of heat flux over the surface, and thus a variable surface velocity. The good agreement with theory suggests that the fuel velocity at the burner face quickly equilibrates to proper diffusional flows in the flame.

Bustamante et al. [4] presented another validation of burner emulation by comparing the flame standoff distance in the laminar region for burning of inclined flat plates. Results showed the similarity in the flame shape for a flat surface oriented at various angles. Even the onset of turbulent unsteady flow was approximately matched.

## 2. Experimental design and testing

Inspired by the de Ris burner, a BRE burner was designed and constructed. Its size was selected to replicate small pool fires. This BRE burner has a face diameter of 50 mm. Its internal features allow for a mixing plenum for the incoming fuel stream, an array of glass beads to provide uniformity to the flow, and a top brass

plate with uniform holes having a high overall porosity. Two heat flux sensors are used anticipating heat flux variation over the surface. They are needed to compute the heat of gasification. Two thermocouples on the operating face record the surface temperature so that the re-radiation heat flux can be computed. Fig. 1 shows the BRE burner with two heat flux sensors, one at the center and the other between the center and edge. The “edge” sensor is at a radius of 3.2 mm. The sensors are 1/8-in. diameter water-cooled Medtherm thermopile devices, operated at about 65 °C to avoid a condensation error. The required heat fluxes needed in Eq. (1) are computed from these temperatures and heat flux measurements. A distribution needs to be postulated to give the integrated average radial heat flux. Also corrections are applied to address the differences in the sensor and plate temperatures. These corrections are generally small, and details will not be presented here.

A series of tests were performed to assess the burner's ability to emulate particular condensed-fuel combustion. The procedure was to measure a steady burning rate for the condensed fuel, then select a gaseous fuel mixture with this same flow rate to best match (1) the heat of combustion, (2) the heat of gasification, (3) the surface temperature, and (4) the laminar smoke point of the original condensed-phase fuel. The heat of combustion and the smoke point could be matched as close as practical by selecting a mixture of pure gaseous fuel and an inert diluent; nitrogen was used.

Several condensed-phase fuels were selected for study: two liquids and two solids. Two of the fuels burn with negligible soot. The four properties were matched as closely as practical, and the burning rates, flame size, character, and color were compared. The burning rate of the condensed fuel is determined by a load-cell measurement of a 50 mm pool fire, and used to fix the BRE flow rate. The liquids were burned in a 50 mm diameter glass vessel. Although the liquid fuel was not refilled during the burning, we have reached the stable burning rate. Literature values are established for the four fuel properties as listed above [5–7]. Two of the four properties – heat of combustion and laminar smoke point – are best matched by selecting the proper gaseous fuel and nitrogen mixture. The other two properties – heat of gasification and surface temperature – are found from the BRE measurements. As the burner surface temperature is not controlled, this matching depends on the burner thermal properties. As long as the surface temperatures are not too out of line, this is not considered a serious defect to the emulation.

The four fuels selected are methanol, heptane, PMMA and POM. The liquids easily ignite and quickly establish steady burning. The solids need to be encouraged to burn, but eventually reach steady conditions.

Methanol was examined first. The mass loss rate of methanol was measured and the flame was photographed. To match the methanol with the BRE we would need to use a gaseous fuel with the same flow rate. To match the flame height, the fuel must have the same heat of combustion. In addition, consideration of the soot

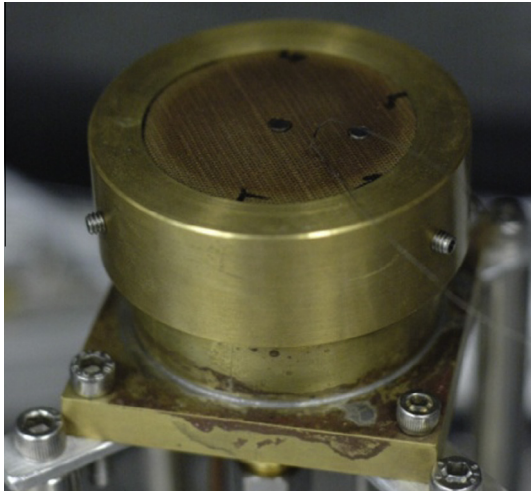


Fig. 1. BRE burner with 50 mm diameter surface.

tendency of methanol led to the choice of methane as the gaseous fuel for the BRE. Nitrogen was added to the fuel stream to match the heat of combustion of methanol, 19.1 kJ/g [6]. The gas burner BRE used a fuel mixture of 52% (volume) methane with 48% nitrogen. The flow rate of the mixture was 24 cc/s to match the burning rate of the methanol at 11 g/m<sup>2</sup> s. If the BRE concept is correct, the two flames should be nearly identical in appearance and in flame heat flux distribution. The measured heat fluxes in the BRE are 5.5 and 21.3 kW/m<sup>2</sup> for the heat flux gages located at the center and at 1.5 cm from the center, respectively. A weighted average over their area segments gives an average value of 15.6 kW/m<sup>2</sup>. Corresponding surface temperature measurements yield an average temperature of 160 °C (141–170 °C). Taking an emissivity of unity for the BRE oxidized porous brass surface, the re-radiative heat flux is approximately 2 kW/m<sup>2</sup>. Consequently, the heat of gasification associated with the BRE as computed from Eq. (1) is  $L = (15.6 - 2 \text{ kW/m}^2) / (11 \text{ g/m}^2 \text{ s}) = 1.24 \text{ kJ/g}$ . The literature value for methanol is 1.20 kJ/g [7]. In addition to small approximations in the calculations, there is a difference of the BRE surface, as it is hotter (160 °C) than the boiling point of methanol at 64 °C. This temperature discrepancy is beyond the control of the BRE, as its surface temperature is a result of the flame and burner heat transfer characteristics.

A visual confirmation of the BRE to emulate the methanol pool fire at 50 mm diameter is shown in Fig. 2a and b, in which the flames are compared when the slightly oscillating images are similar. The color, size, and oscillatory character are similar.

We then sought to evaluate whether the burner could also emulate other burning conditions. We considered a 50-mm-diameter burning pool of heptane. Here the flame would be yellow from soot. The choice of the gaseous fuel in the BRE was again made by matching the heat of combustion and the laminar smoke point for heptane. Ethylene was selected to be used as the burner gas to simulate heptane. The heat of combustion of ethylene is close to that of heptane (41.5 kJ/g compared to 41.2 kJ/g) [6], as is the laminar smoke point (120 mm compared to 139 mm) [8]. A visual confirmation for the nature of these turbulent heptane flames is shown in Fig. 3.

Two solids were then examined: PMMA and POM. The latter burns with negligible soot. A propylene and nitrogen mixture (50% in mole fraction) was used to emulate PMMA. Steady burning of the PMMA was achieved by igniting it in an inverted orientation (facing down) and allowing the flame to stabilize, after which the sample was oriented as a pool fire where it sustained steady

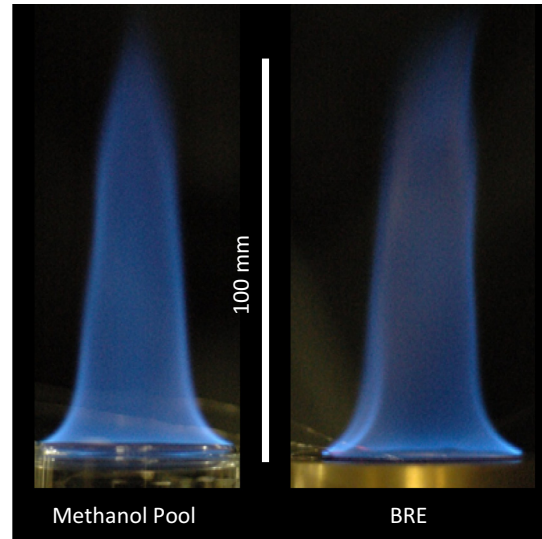


Fig. 2. Comparison of 50 mm diameter methanol flame reproduced by the BRE burner.

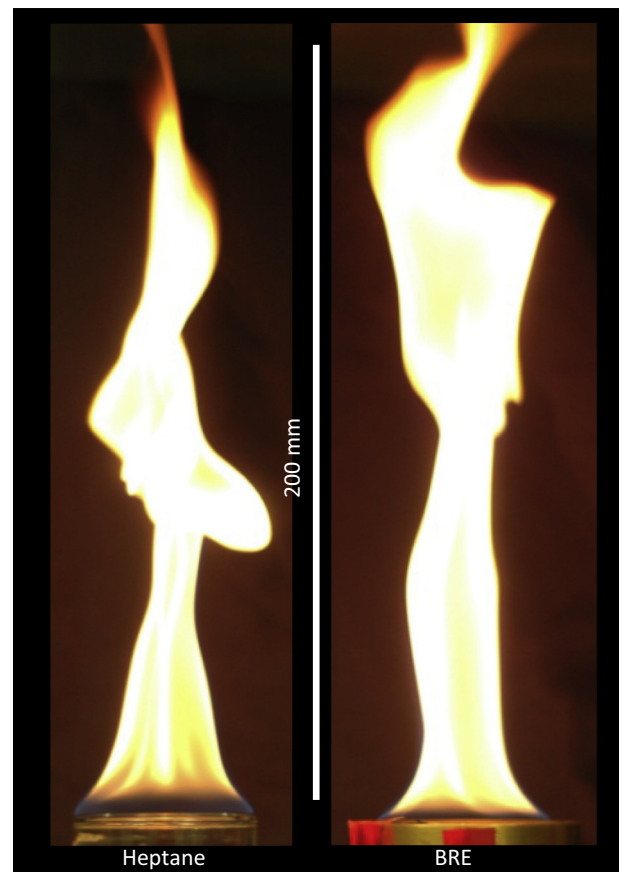


Fig. 3. Comparison of 50 mm diameter heptane flame reproduced by the BRE burner.

burning. A visual confirmation for the comparison of PMMA and BRE is shown in Fig. 4.

The results for POM are shown in Fig. 5. As with the PMMA, the POM was cut to 50 mm diameter disk. Before placed on a scale, it was first heated with pilot flame until the flame covered the whole burning surface. The POM burnt steadily and that value was

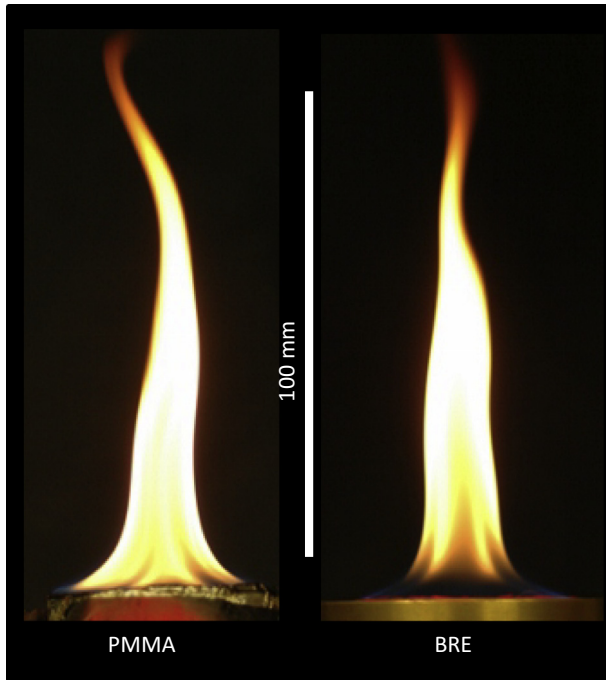


Fig. 4. Comparison of 50 mm diameter PMMA flame reproduced by the BRE burner.

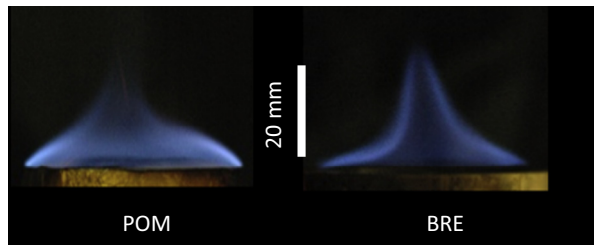


Fig. 5. Comparison of 50 mm diameter POM flame reproduced by the BRE burner.

matched by the BRE. The color and nature of the BRE flame is well matched by the POM mixture. The relevant properties are given in Table 1 along with those of the other fuels. The BRE cannot match the surface temperature, but more importantly the heat of gasification is nearly matched in all cases. These examples confirm the implicit hypothesis of the four properties being sufficient to establish the same burning condition with the BRE.

### 3. Difficulties

It should be noted that the demonstration of the BRE to emulate real fuel fires is not without difficulties. The burning of small pool

fires of 50 mm diameter is fraught with issues. It is known that for liquid pools edge heat losses to the container, and the container lip influence the burning rate. Also refilling the liquid to maintain a fixed level has an effect. Many investigators have tried to minimize these issues. Yet, as seen for example in Fig. 6, the burning rates presented in the literature for methanol, including ours, have differences [8–11].

In addition, the BRE uses two point heat flux measurements to obtain the average net heat flux required by Eq. (1). To be accurate, these points must be incorporated into a proper distribution across the radius of the burner. Theory or experimental results can guide this. Unfortunately there has been little done in this area. The work of Akita and Yumoto [8] shed some light on the heat flux distribution. They measured the burning rate in small pool fires over three concentric regions of the pool. From this the heat flux can be deduced, and the results are shown in Fig. 7. It is shown that the related heat flux distribution can be exponential over the radius. (Note the heat flux is proportional to the supply velocity, Eq. (1)). This sharp increase in heat flux to the edge can be appreciated by examining the flame shape for ethylene as shown in Fig. 8. Two features should be noted, (1) the closeness of the flame at the edge giving high convection heat transfer, and (2) the color of the body of the flame indicating the presence of radiation.

In processing the data for the four fuel emulations, the heat flux was assumed to step change for the two sensors. This is shown by

$$\begin{aligned}\dot{q}_{avg}'' &= \frac{1}{\pi 2.5^2} \int_0^{2.5} \dot{q}'' 2\pi r dr = \dot{q}_{r=0}'' \left(\frac{1.5}{2.5}\right)^2 + \dot{q}_{r=1.5}'' \left(1 - \frac{1.5}{2.5}\right)^2 \\ \dot{q}_{avg}'' &= 0.36\dot{q}_{r=0}'' + 0.64\dot{q}_{r=1.5}''\end{aligned}\quad (3)$$

Obviously the nature of the distribution is key to interpreting the two sensors. We are continuing to work this issue and are currently in the process of measuring a more complete distribution with an array of sensors. Just to show the differences that can be developed, we compare the individual sensors, with the distribution in Eq. (3), and the average heat flux measured by a perforated relatively thick copper exit plate for the burner. This top plate is used as a calorimeter, and its heat flux is deduced by a heat transfer analysis. This has been incorporated into a new burner design, and it is still under development. As we assure its accuracy, we would now have a way to derive the average as well as two point measurements for the heat flux. A preliminary result is shown in Fig. 9. The figure shows that the heat flux tends to become more uniform as the burning rate increases. The average heat flux decreases less with increasing mass transfer. This suggests that the peak heat flux occurs at larger radii with increasing mass flux. This is expected as the flame is pushed farther away from the surface. The results show the top plate calorimeter is about 15% higher than that using Eq. (3).

These difficulties suggest that the very good results for the emulation in Table 1 could be fortuitous. However, it should be realized that the BRE is matching the burning rate obtained in

Table 1  
Literature [6–8] and measured properties that determine the burning conditions.

		$\dot{m}''$ (g/m <sup>2</sup> s)	$\Delta h_c$ (kJ/g)	SP (mm)	$T_s$ (°C)	$L$ (kJ/g)
Methanol	Pool	11	19	$\infty$	64	1.2
	BRE ( $X_{CH_4} = 52\%$ , $X_{N_2} = 48\%$ )	11	19	$\infty$	160	1.24
Heptane	Pool	15	41.2	139	98	0.48
	BRE ( $C_2H_4$ )	15	41.5	120	211	0.51
PMMA	Pool	6	24.2	105	390	1.6
	BRE ( $X_{C_3H_6} = 50\%$ , $X_{N_2} = 50\%$ )	6	24.3	117	312	1.8
POM	Pool	9	14.4	$\infty$	420	2.4
	BRE ( $X_{CH_4} = 41\%$ , $X_{N_2} = 59\%$ )	9	14.1	$\infty$	167	2.1

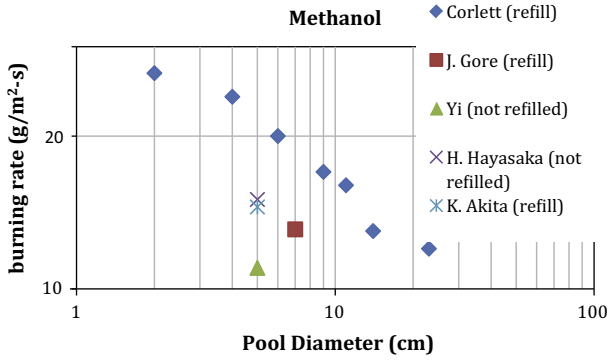


Fig. 6. Burning rates of methanol pool fires of small diameter [8,9].

our experiments though they might not be the most accurate steady state results. Also the two-point integration to get the average heat flux might be satisfactory, with a 15% possible error, but our evaluation is still in progress. Yet the color and height of the flames add to the credibility of the BRE. Moreover, past work supports its performance [1–4].

4. Other applications for the BRE

Having demonstrated the BRE’s capability to emulate the combustion of various fuels in normal gravity, extensions of its use can be considered. It provides a very controllable way to study steady burning. Its configuration and size can be varied. It can be used in many different environments.

As in the studies by de Ris et al. [1–3], the burner can be operated over a range of  $L$  or  $B$  values. This is particularly applicable to purely convective burning. We demonstrated this for the 50 mm BRE using a mixture of methane and nitrogen to generate data over a range of  $B$  values. The results correlated with  $\ln(1+B)$  giving a convective heat transfer coefficient of  $10.5 \text{ W/m}^2 \text{ K}$  are plotted in Fig. 10. Along with the data of the BRE with diluted methane, several real condensed fuels were added. As methane tends to have a relatively low radiation loss, as well as methanol, the PMMA and heptane having higher radiative losses could explain their variation. The higher the radiation loss, the lower the flame temperature and for a small diameter pool where convection dominates, the burning rate is apt to be lower as shown on the graph.

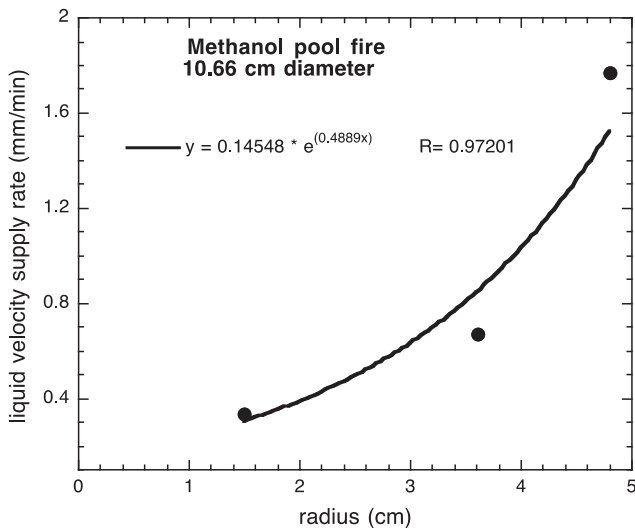


Fig. 7. Methanol supply rates over three concentric section of a 10.66 cm diameter pool fire (from [8]).



Fig. 8. Ethylene flame on the BRE 50 mm burner.

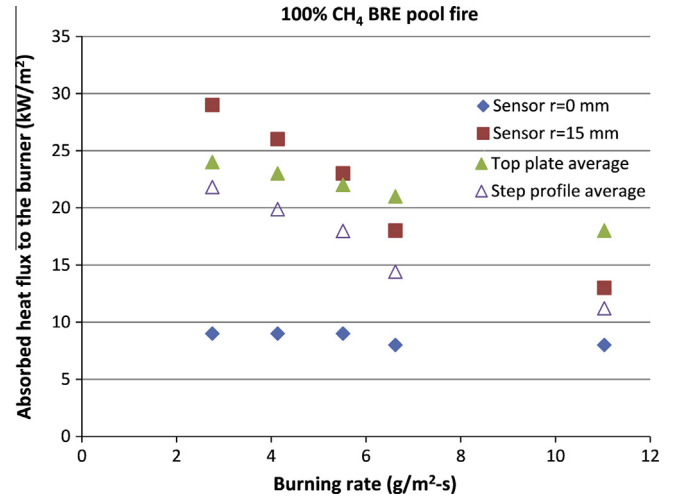


Fig. 9. Heat flux to the 50 mm BRE as a function of flow rate of pure methane.

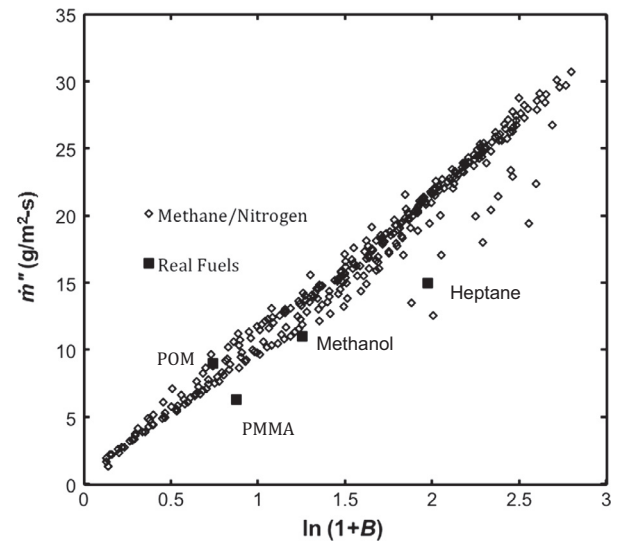


Fig. 10. BRE steady burning for  $\text{CH}_4\text{-N}_2$  mixtures at 50 mm and “real” solid/liquids.

Mass-loss flux at ignition and extinction limits are important properties of fires. Yet their evaluation for condensed fuels is difficult to capture because of their highly transient nature. Materials experience a sudden jump in mass-loss rate when ignited or when they suddenly extinguish. Such transients are difficult to accurately measure. By using the BRE, the mass-loss rate can be clearly identified by increasing the flow rate of fuel gradually until the sustained ignition is observed, or decreasing it to extinction after a flame is sustained.

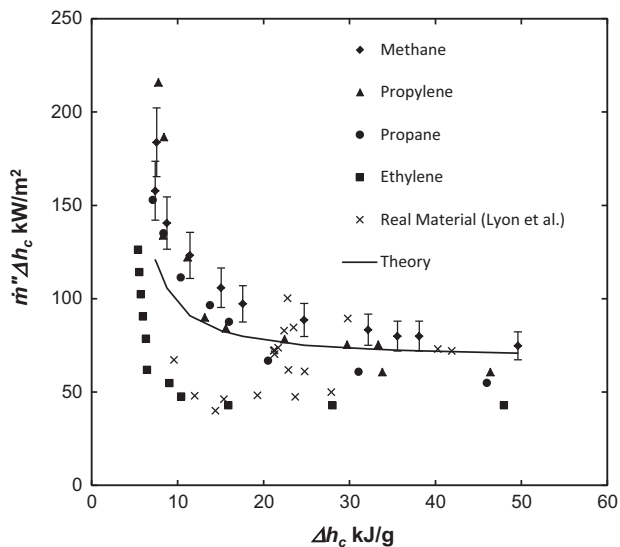


Fig. 11. Extinction conditions for various solid fuels and data from the BRE for several gaseous fuels [12].

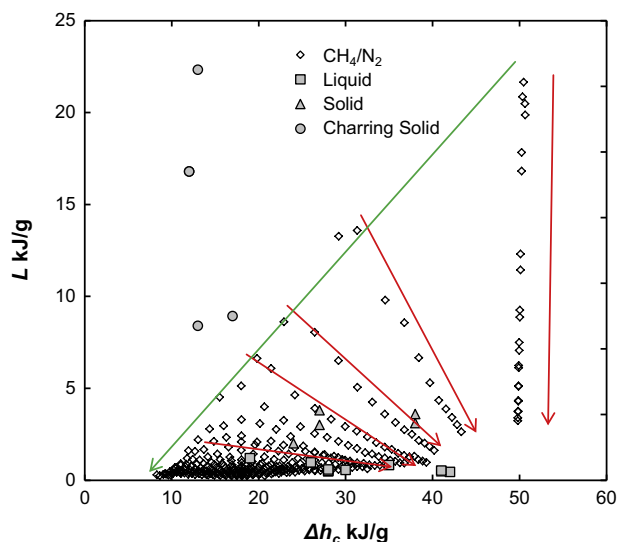


Fig. 12. Flammability map by BRE in normal gravity (arrows toward the right fix the nitrogen flow rate and increase the methane flow rate from 0 to 2 slpm). The boundary with the arrow to the left is close to the fire point data for the fuel mixture.

Lyon and Quintiere [12] compiled extinction data for condensed fuels and examined their dependency with the heat of combustion. Those data are compared in Fig. 11 for four gaseous fuels mixed with nitrogen in the BRE. As the fuels have differing laminar smoke points, the trends differ for each and suggest an effect of radiation. The theoretical curve is taken from the analysis in [12]. We are in the process of further studying these limits.

The BRE can be used with various fuel mixtures to prescribe the heat of combustion and laminar smoke point. Over a range of flow rates where a steady flame is sustained, the BRE then establishes the corresponding heat of gasification and burning temperature. These burning points can be plotted in a multi-dimensional format to display the range of conditions that support steady burning. Fig. 12 is a sample of such a plot in two dimensions that shows the steady state domain of the 50 mm BRE in air with coordinates of heat of combustion and heat of gasification. Re-radiation heat flux and laminar smoke point are ignored here, but must be

considered to be complete. In contrast to the steady domain of the BRE results, data for solids and liquid fuels are included. The charring materials lie outside of the “flammability” domain, and are well known not to burn without the support of external heating or increased ambient oxygen. Liquid fuels and non-charring solids do fall within the flammability domain as might be expected. A study along these lines is ongoing, and it will be challenging on how to present it, verify it, and explain it.

## 5. Conclusions

The BRE is capable of matching the burning rate and flame characteristics of a condensed-phase fuel by maintaining the heats of combustion and gasification, burning surface temperature and the laminar smoke point the same, as practicable. This has been demonstrated for pool fires of methanol, heptane, PMMA, and POM. However even with the success of these demonstrations, questions exist about the interpretation of the heat flux distribution, and on the accuracy of the burning rate measured for the comparable pool fires. No good data or any theory exists for pool fires, particularly in the range of 25–100 mm in diameter. Nevertheless the BRE concept allows for a more careful vehicle for the study of these features over the difficulties with burning condensed-phase fuels. We are engaged in work to measure the average heat flux to the burner by means of a top-plate calorimeter, in addition to point measurements. The ability to compute an accurate heat of gasification for the BRE depends on obtaining this average heat flux determination.

Extinction and ignition conditions for the burning of condensed-phase fuels can be studied much more easily and accurately with the BRE. While standard tests exist for measuring the flash and fire-point of liquid fuels, they do not yield the mass flux for these conditions. Modelers are currently using such critical mass flux values to predict the ignition of solids. The BRE is capable of giving this value in a precise and well-defined manner. Definitions of the flash, fire and extinction points can be sharp with the BRE. In our ongoing studies, the BRE demonstrates that the fire and extinction points do not necessarily have full fuel diameter flames at these transitions. For solids and liquid fuel fuels such transitions are very transient and rapidly move from full flame to no flame, or vice versa. The BRE allows a steady snapshot study of these transitions. Work is ongoing to elucidate and measure these transition points, and hopefully to more fully demonstrate their dependence on the heat of combustion.

The BRE offers a convenient way to study the prospect of steady burning in various ambient conditions including microgravity. Of course experiments in microgravity must be done in orbit to allow sufficient time to reach valid end states. However studies with the BRE in 5 s drop experiments have given interesting results. Although the flames are still slowly evolving at the end of the microgravity drop, a steady state convective theory was capable for correlating the burning rate and final size of the flames over a range of  $B$  numbers [13].

In conclusion, the concept of the BRE defined herein offers a platform for the study of diffusion flames related to real condensed-phase fuels. It offers advantages by allowing steady conditions to prevail long enough to make detailed measurements of variables of interest, and to better defined the limits of burning at ignition and extinction.

## Acknowledgment

This work was funded by NASA Grant NNX10AD98G for which Paul Ferkul and Dennis Stocker have served as the technical contact, and have provided important support.

**References**

- [1] L. Orloff, J. de Ris, *Proc. Combust. Inst.* 13 (1971) 979–992.
- [2] J.S. Kim, J. de Ris, W.F. Kroesser, *Proc. Combust. Inst.* 13 (1971) 949–961.
- [3] J. de Ris, L. Orloff, *Proc. Combust. Inst.* 15 (1975) 175–182.
- [4] M.J. Bustamante, K.T. Dotson, Y. Zhang, P.B. Sunderland, J.G. Quintiere, *Laminar Burning on Flat Wicks at Various Orientations*, Spring Technical Meeting of the Central States Section of the Combustion Institute, 2012.
- [5] Y. Zhang, M.J. Bustamante, M.J. Gollner, P.B. Sunderland, J.G. Quintiere, *J. Fire Sci.* 32 (2014) 52–71.
- [6] J.G. Quintiere, *Fundamentals of Fire Phenomena*, John Wiley & Sons Ltd., Chichester, U.K., 2006.
- [7] L. Li, P.B. Sunderland, *Combust. Sci. Technol.* 184 (2012) 829–841.
- [8] K. Akita, T. Yumoto, Heat transfer in small pools and rates of burning of liquid methanol, *Proc. Combust. Inst.* 10 (1965) 943–948.
- [9] R.C. Corlett, T.M. Fu, Some recent experiments with pool fires, *Pyrodynamics* 1 (1966) 253–269.
- [10] H. Hayasaka, Unsteady burning rates of small pool fires, *Fire Saf. Sci.* 5 (1997) 499–510.
- [11] J. Gore, M. Klassen, A. Hamins, T. Kashiwagi, Fuel property effects on burning rate and radiative transfer from liquid pool flames, *Fire Saf. Sci.* 3 (1991) 395–404.
- [12] R.E. Lyon, J.G. Quintiere, *Combust. Flame* 151 (2007) 551–559.
- [13] Yi Zhang, Matt Kim, Haiqing Guo, Peter B. Sunderland, James G. Quintiere, John deRis, Dennis P. Stocker, Emulation of condensed fuel flames with gases in microgravity, *Combust. Flame* 162 (2015) 3449–3455.